

## The structure of the clean Mo{001} surface

A. Ignatiev,\* F. Jona, and H. D. Shih

*Department of Materials Science, State University of New York, Stony Brook, New York 11794*

D. W. Jepsen and P. M. Marcus

*IBM Watson Research Center, Yorktown Heights, New York 10598*

(Received 24 February 1975)

An analysis of low-energy-electron-diffraction data from a clean Mo{001} surface was carried out, which has determined the atomic structure of this surface and provided the parameters of a scattering model needed to analyze ordered overlayers. The analysis was based upon the comparison between the intensity spectra calculated with the layer-Korringa-Kohn-Rostoker method and the spectra determined experimentally for six nondegenerate diffracted beams at 8° and four nondegenerate diffracted beams at 21° incidence of the primary electron beam. Satisfactory fit to experimental spectra was obtained with a model using an energy-dependent inner potential varying from 16 to 13 eV, an imaginary potential of 4 eV, bulk and surface Debye temperatures of 360 and 150°K, and a first underlayer spacing of 1.39 Å; thus the Mo{001} surface is contracted by 11.5% with respect to bulk {001} planes. The sensitivity of the calculated spectra to changes in a number of structural and nonstructural model parameters is demonstrated and discussed.

### I. INTRODUCTION

The structures of clean nonreconstructed metallic surfaces have been the object of several investigations in recent years by low-energy-electron diffraction (LEED).<sup>1</sup> These investigations have usually had three objectives which also motivated the present work: (i) to test methods and procedures of surface-structure analysis on relatively simple models involving no rearrangements of atoms within the plane of the surface; (ii) to examine the effects of crystal termination on the uppermost layer(s) of atoms; (iii) to prepare for studies of usually more complex overlayer structures that are obtained by reactions of the clean surfaces with gases or vapors. The present study of the clean {001} surface of molybdenum is the first detailed structure analysis by LEED of a surface of a bcc metal. In Sec. II, we describe the experimental procedures followed for cleaning the surface and for collecting the data to be used in the structure analysis. In Sec. III, we present the results of model calculations, examine the effects of parameter changes and compare calculated with observed data. In Sec. IV, we discuss the results of the structure analysis and summarize the conclusions.

### II. EXPERIMENTAL PROCEDURES

The single-crystal slug from which the samples were obtained had a quoted purity of 99.992% (source: Materials Research Corp., Orangeburg, N. Y.). Platelets were cut with their major surfaces perpendicular to a  $\langle 100 \rangle$  direction within an accuracy of  $\pm 0.5^\circ$ , lapped and mechanically polished according to standard metallographic procedures. The final samples were about  $2 \times 0.5$

$\times 0.025$  cm in size, the {001} surface being polished to mirror finish with only a few scratches. No chemical treatments of the surface were attempted. A platelet was mounted in the appropriate sample holder,<sup>2</sup> inserted in the vacuum system and, after attainment of base pressure ( $\sim 1 \times 10^{-10}$  Torr), subjected to 4-h argon-ion bombardment (600 V,  $4 \mu\text{A}/\text{cm}^2$  at  $1 \times 10^{-4}$  Torr of Ar gas) prior to any heating. The chemical composition of the surface was monitored by Auger-electron spectroscopy (AES). The most abundant and tenacious contaminant was found to be carbon, probably diffusing onto the surface from the bulk. A series of treatments involving 3-h ion bombardment followed by 10-min anneals at 800 °C for a total of 24 h failed to remove the carbon signal from the AES scan. Additional 10-h ion bombardment of the hot sample ( $\sim 800^\circ\text{C}$ ) also failed to eliminate the carbon signal. Heating of the sample to 1400 °C in  $5 \times 10^{-6}$  Torr of oxygen for 3-h removed the carbon peak from the AES scan but caused the appearance of a pronounced oxygen peak. The oxygen contamination was only slightly decreased (by about 15%) by a heating treatment of the sample at 1400 °C for 6 h *in vacuo* ( $5 \times 10^{-10}$  Torr) and more strongly reduced by a series of argon-ion bombardments followed by anneals for a total of 5 h. However, the reduction of the oxygen peak from the AES trace was accompanied by a reappearance of the carbon peak. Fortunately, it was observed at this stage that ion bombardment at about  $45^\circ$  to the platelet surface increased markedly the efficiency of carbon removal. This effect was probably due to the low-sputtering yield of C with respect to Mo, which for ion bombardment at normal incidence may cause the formation of Mo pillars or hillocks with the tops covered by

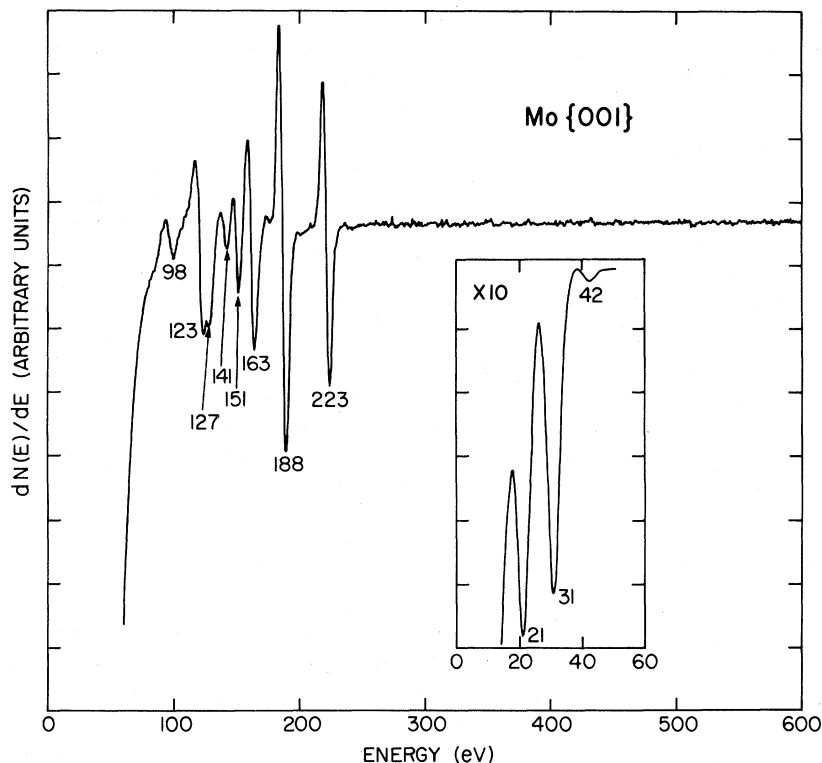


FIG. 1. Auger spectrum of clean Mo{001}. Exciting electron beam: 3000 V, 50  $\mu$ A. Modulating voltage: 5 V peak to peak for the large scan, 2 V peak to peak for the curve in insert.

C atoms.<sup>3</sup> In this case, ion bombardment at 45° to the surface is indeed expected to be more successful in eliminating both the impurity atoms and the irregularities of the surface. In fact, alternate room-temperature ion bombardments at 45° followed by anneals for a total of 30 h succeeded in producing a clean Mo{001} surface. The AES scan obtained at the end of the cleaning process is depicted in Fig. 1. After the clean-surface condition was attained, the recleaning procedure which is required prior to collection of intensity data consisted routinely of 1-h ion bombardment at room temperature followed by 8-min anneal at 1000 °C.<sup>4</sup>

It should be noted here that some controversy has existed in the literature regarding the nature of the 141 and 151 eV peaks in Mo AES spectra.<sup>5,6</sup> Our analysis indicated that these peaks are in fact due to molybdenum and not to a sulfur impurity. The presence of a sulfur impurity was initially observed on the Mo surface as a single strong peak (AES peak-to-peak height equal to that of the 188-eV Mo peak) at 150 eV. However, after approximately 2-hrs of ion-bombardment, the 140–190-eV region of the AES spectrum was identical to that of Fig. 1 (the scan of Fig. 1 was taken after about 75 h of ion-bombardment) with the relative intensities of the 141- and 151-eV peaks in the ratios of 1:10 and 1:4.5 to the intensity of the 188 eV Mo peak. The invariance of the 141/188 and 151/188 peak ratios with respect to surface clean-

ing procedures, and the appearance of a single strong peak at 150 eV upon sulfur contamination indicate that the 141- and 151-eV peaks in the Mo AES spectrum are indeed molybdenum peaks.

The LEED observations and measurements were made within a conventional four-grid display system. The intensities of the diffracted beams were determined from the brightnesses of the corresponding spots on the fluorescent screen. The response of the photometer used for the brightness measurements was calibrated with a movable Faraday cage inside the vacuum system. The zeros of the angle  $\theta$  between the incident electron beam and the normal to the sample surface, and of the angle  $\phi$  between the projection of the incident beam on the sample surface and the  $k_x$  axis (defined as the axis from the 00 beam to the 10 beam) were determined with procedures described earlier.<sup>7</sup> Residual magnetic fields in the LEED chamber were minimized with three mutually-perpendicular sets of Helmholtz coils. In order to make all diffracted beams visible on the fluorescent screen from emergence, the sample was biased negatively (–150 V) with respect to the first grid of the LEED optics.

During the annealing cycles, the sample was heated resistively and for this purpose, pressure contacts were provided at both ends of the platelet-like sample. Provisions were made for thermal expansion of the sample during the annealing cy-

cles. Nevertheless, at the end of the run, the sample was found to be noticeably buckled, undoubtedly as a consequence of partial failure of the thermal-expansion compensating scheme during the very numerous heating and cooling cycles required by the cleaning process (see above). It was impossible to determine exactly at what stage of the run the deformation of the sample surface occurred, but the incident may conceivably have affected some of the experimental data discussed below.

The structure analysis described in the following is based on two sets of experimental intensity data, one set consisting of six nondegenerate diffracted beams (00, 10,  $\bar{1}0$ , 0 $\bar{1}$ ,  $\bar{1}\bar{1}$ , 11) at  $\theta = 8^\circ$  and  $\phi = 0^\circ$ , the other set consisting of four nondegenerate diffracted beams (00,  $\bar{1}0$ , 01,  $\bar{1}\bar{1}$ ) at  $\theta = 21^\circ$  and  $\phi = 0^\circ$ . All experimental curves presented below (except those in Fig. 5) have been normalized to constant incident-electron current and corrected for a contact-potential difference of 3.2 eV (calculated from the work functions 4.4 eV of Mo{001} (Ref. 8) and 1.2 eV of the filament employed).

### III. STRUCTURE ANALYSIS

The analysis was carried out by comparing with experiment the diffracted-intensity-versus-energy curves (spectra) calculated for specific models. A model is defined by a set of *structural* parameters (involving the positions of atoms relative to one another) and a set of *nonstructural* parameters (involving the real and the imaginary part of the crystal potential in the bulk and at the surface, and the mean square amplitudes of lattice vibrations in the bulk and at the surface). The calculations were done with the layer-KKR (Korringa-Kohn-Rostoker procedure described<sup>9</sup> and applied successfully to surfaces of fcc metals<sup>10</sup> in earlier publications, and used eight phase shifts over the energy range 0–150 eV and 29 beams in the representation of the wave function.

The initial values of the nonstructural parameters

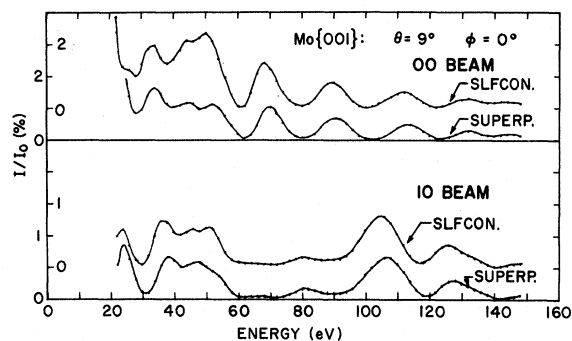


FIG. 2. Comparison between LEED spectra calculated for Mo{001} with a "selfconsistent" (slfcon.) and a "superposition" (superp.) potential. For definitions of terms, see text.

were chosen from available or otherwise estimated data applicable to molybdenum. The "inner potential"  $V_0^B$  (equivalent to the spatially averaged potential between the atoms in the crystal referred to vacuum) was estimated from the known position of the Fermi level with respect to the muffin-tin zero and the measured-static work function. The corresponding surface value  $V_0^S$  was set equal to  $V_0^B$ . The Debye temperature  $\Theta_D^B$  of the bulk was fixed at 360 °K from x-ray data and the corresponding surface quantity  $\Theta_D^S$  was set equal to  $\Theta_D^B$ . The value of the imaginary part  $\beta^B$  of the potential in the bulk was estimated from experience with other metals<sup>10</sup> at about 4 eV, and the corresponding surface quantity  $\beta^S$  was again set equal to the bulk value. For the real part of the potential, we chose the band-structure potential calculated selfconsistently for a muffintin potential. We call this potential a "selfconsistent potential" to distinguish it from the simpler "superposition potential" that constitutes the starting point of the iteration process leading to selfconsistency and is obtained by superposition of atomic charge densities. In order to answer the obvious question about the difference between the two from the point of view of LEED applications, we have calculated several spectra with both potentials and compared the results. The differences were found to be negligible. Figure 2 depicts 00 and 10 spectra, both calculated with the selfconsistent and the superposition potentials. These spectra were chosen for display because they show some of the most pronounced difference encountered. In fact, we note some differences in relative peak intensities for both spectra in the energy range between 30 and 60 eV, and some small shifts (about 2 eV) in peak positions around 70 eV for 00 and 105 eV for 10, but in general corresponding spectra were found to be very similar to one another—most differences are smaller than those found between theory and experiment in a "successful" structure analysis. We conclude, therefore, that either "selfconsistent" or "superposition-type" band-structure potentials can be used for LEED calculations with equally good results.

The imaginary part  $\beta^B$  of the bulk potential can be determined as a function of the incident-electron energy with a method, described elsewhere,<sup>11</sup> that involves measurement and calculations of the total electron current reflected elastically by the sample surface. This method was applied to the present case of Mo{001}, but since it was found that  $\beta^B$  fluctuates consistently around the value of 4 eV between approximately 35 and 150 eV (the range of incident-electron energies considered in this analysis), it was decided to maintain  $\beta^B$  constant at 4 eV for all calculations to follow.

The set of *structural* parameters needed by the

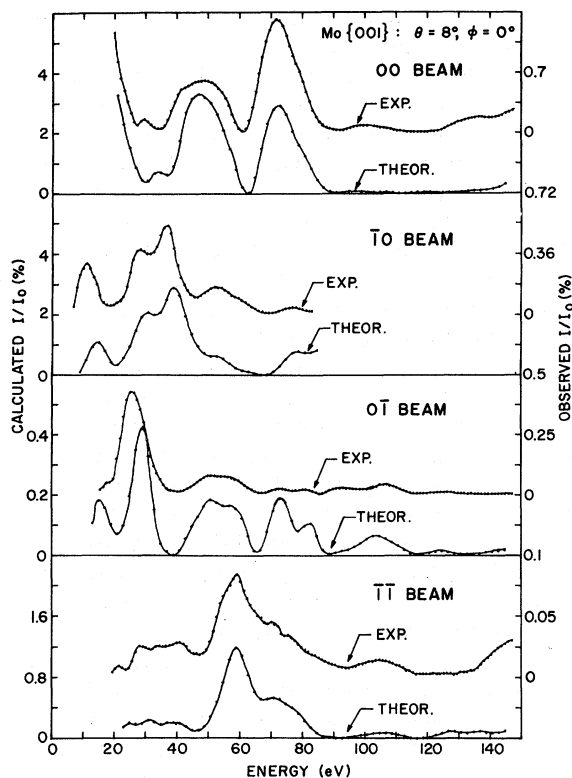


FIG. 3. 00,  $10$ ,  $0\bar{1}$  and  $1\bar{1}$  spectra of Mo{001} for  $\theta = 8^\circ$ ,  $\phi = 0^\circ$  observed and calculated for a surface interplanar spacing  $d_z^S = 1.47 \text{ \AA}$ .

model for the Mo{001} surface contains initially only one unknown, namely, the distance  $d_z^S$  between the top layer of atoms and the layer immediately underneath (the coordinates of each top-layer atom *within* the plane of the layer are fixed by the requirement of registry with the structure of the bulk). The intensity calculations were thus carried out for a number of  $d_z^S$  values varied around the bulk value  $d_z^B = 1.57 \text{ \AA}$  of the interplanar distance along  $\langle 001 \rangle$ . It appeared clear almost immediately that values of  $d_z^S$  close to  $d_z^B$  produce

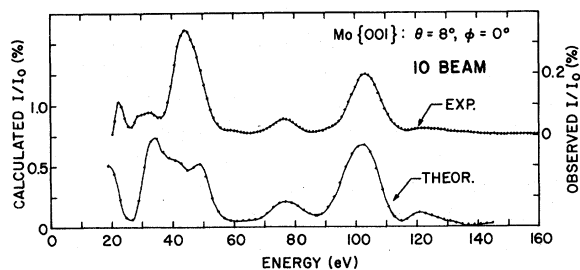


FIG. 4.  $10$  spectrum of Mo{001} for  $\theta = 8^\circ$ ,  $\phi = 0^\circ$  observed and calculated for a surface interplanar spacing  $d_z^S = 1.47 \text{ \AA}$ . In the energy range between 30 and 60 eV, the theory predicts three peaks, while the experiment reveals only two.

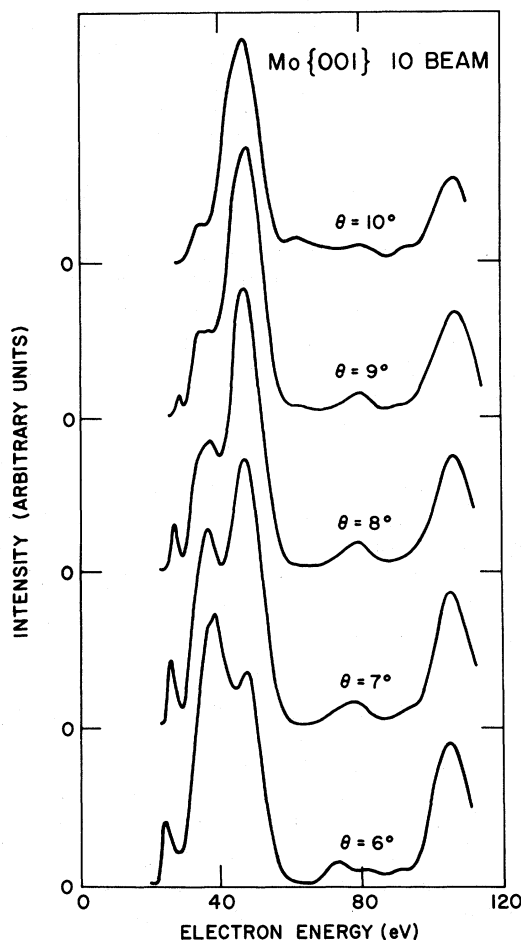


FIG. 5. Experimental  $10$  spectra (not normalized) from clean Mo{001} as functions of the angle of incidence  $\theta$  of the primary electron beam.

satisfactory correspondence between calculated and observed LEED spectra for some beams but not for others. Figure 3 depicts experimental and theoretical  $00$ ,  $10$ ,  $0\bar{1}$  and  $1\bar{1}$  spectra (calculated for  $d_z^S = 1.47 \text{ \AA}$ ) in acceptable agreement with one another, but Fig. 4 shows that for the  $10$  beam, the correspondence between observation and calculation, while good above 60 eV, is not satisfactory between 30 and 60 eV. In this energy range, the calculated curve exhibits three peaks, while the experiment records only one small peak around 30 eV and one tall peak at about 44 eV.

In situations of this kind it is reasonable to question first the veracity of the experimental data, particularly because the quoted value of the angle of incidence  $\theta$  is expected to be accurate only within approximately  $2^\circ$ . For this reason, we examined the angular dependence of the experimental  $10$  spectrum in the range between  $\theta = 6^\circ$  and  $\theta = 10^\circ$ . The results, depicted in Fig. 5 in non-normalized form, show clearly that between 30 and 60 eV,

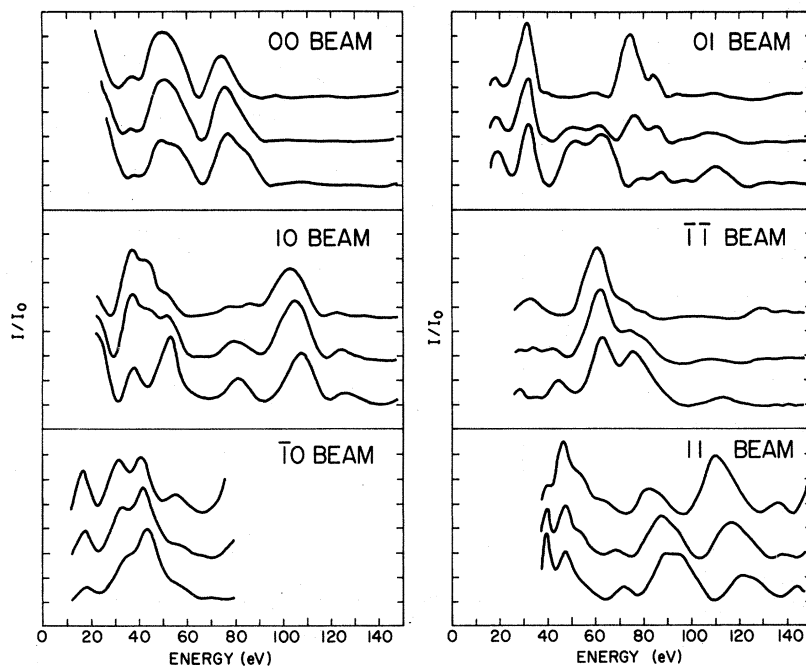


FIG. 6. Calculated spectra for six nondegenerate beams from a model Mo{001} surface. In each panel, the top curve was calculated for a surface interplanar spacing equal to the bulk,  $d_z^S = d_z^B = 1.57 \text{ \AA}$ ; the middle curve was calculated for  $d_z^S = 1.47 \text{ \AA}$  (6.4% contraction), and the bottom curve for  $d_z^S = 1.36 \text{ \AA}$  (13.4% contraction).

there are always only two peaks, although their relative intensities vary markedly with  $\theta$ . We proceeded therefore to examine systematically the dependence of the calculated spectra upon the parameter  $d_z^S$ . Figure 6 summarizes the results of this study for all six beams considered in the present analysis: In each panel we present three curves for one beam, the top curve calculated for  $d_z^S = d_z^B = 1.57 \text{ \AA}$ , the middle curve for  $d_z^S = 1.47 \text{ \AA}$  (corresponding to 6.4% contraction of the top atomic layer), and the bottom curve for  $d_z^S = 1.36 \text{ \AA}$  (13.4% contraction). It is clear that while all spectra exhibit some changes with  $d_z^S$ , none is as sensitive to this parameter as the 10 spectrum in the energy range from 30 to 60 eV. For all other spectra, it can be said that some peaks vary markedly in relative intensity (O1 beam), and some vary slightly in position (11 beam) as  $d_z^S$  is changed, but only in the 10 spectrum do we observe that three adjacent peaks are reduced to two with increasing  $d_z^S$ . Careful scrutiny revealed that values of  $d_z^S$  corresponding to at least 10% contraction of the top layer are necessary in order to reproduce the shape of the experimental 10 beam curve. Best over-all agreement between observed and calculated spectra was found for  $d_z^S = 1.39 \text{ \AA}$ , corresponding to 11.5% contraction of the top interplanar spacing with respect to the bulk.

At this stage of the analysis, with the structural problem essentially solved, it was appropriate to examine the effects of changes in the nonstructural parameters that were still available for adjustments. Figure 7 shows the effect of changes in the

Debye temperature  $\Theta_D^S$  of the surface layer. In general, it was observed that substantial decrease of the  $\Theta_D^S$  value ( $\Theta_D^B$  remaining fixed at 360 °K) enhanced the heights of higher-energy peaks over those of lower-energy peaks. Although the differences between spectra calculated with different values of  $\Theta_D^S$  were found to be minor, it was concluded that the correspondence between theory and experiment for all six beams considered was slightly improved by the choice  $\Theta_D^S = 150 \text{ °K}$ . Surface Debye temperatures lower than bulk Debye

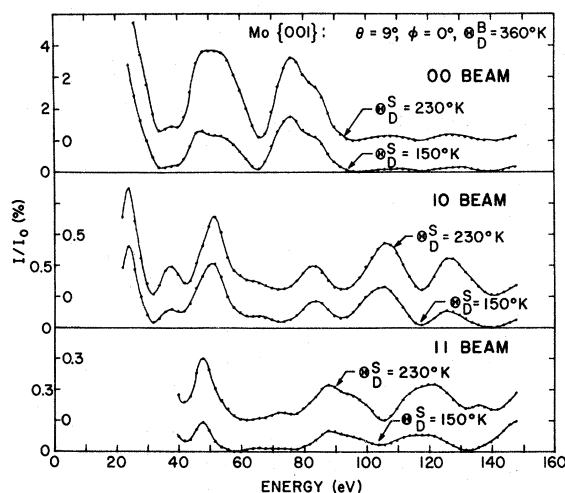


FIG. 7. Effect of changes in the surface Debye temperature  $\Theta_D^S$  for fixed bulk Debye temperature  $\Theta_D^B$  on three LEED spectra from a model Mo{001} surface.

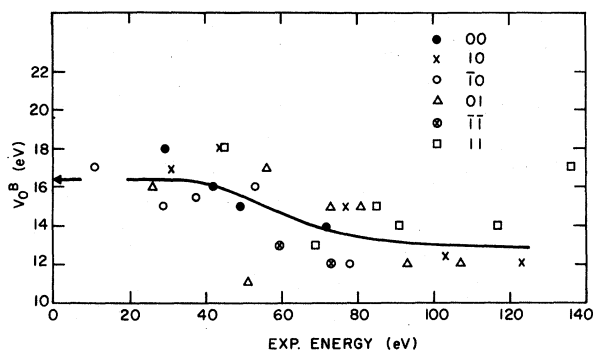


FIG. 8. Dependence of the bulk "inner potential"  $V_0^B$  for clean Mo{001} upon energy. The value indicated by the arrow represents the sum of work function and Fermi level with respect to the muffin-tin zero for the selfconsistent potential used in the calculations.

temperatures have been measured<sup>12-17</sup> and discussed<sup>18-20</sup> by several workers. The value  $\Theta_D^S = 150^\circ\text{K}$  used here is consistent with direct measurements of the effective-surface Debye temperature of clean Mo{001} by Tabor *et al.*<sup>5</sup>

The value of the bulk inner potential  $V_0^B$  can be determined more accurately than was done initially, particularly in its dependence upon electron energy, by measuring the shifts that would be required in order to match the peak positions in a spectrum

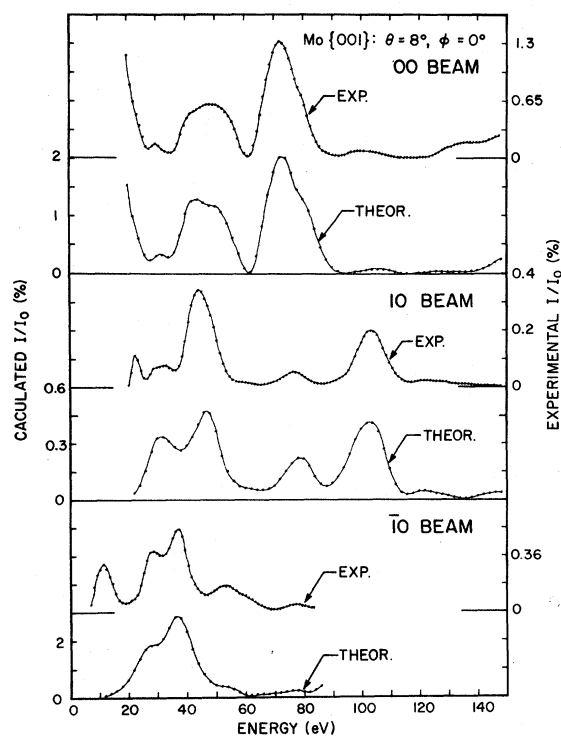


FIG. 9. Experimental and theoretical spectra (calculated with the parameters listed in the text) for clean Mo{001} at  $\theta = 8^\circ$ ,  $\phi = 0^\circ$ ; 00, 10 and  $\bar{1}0$  beams.

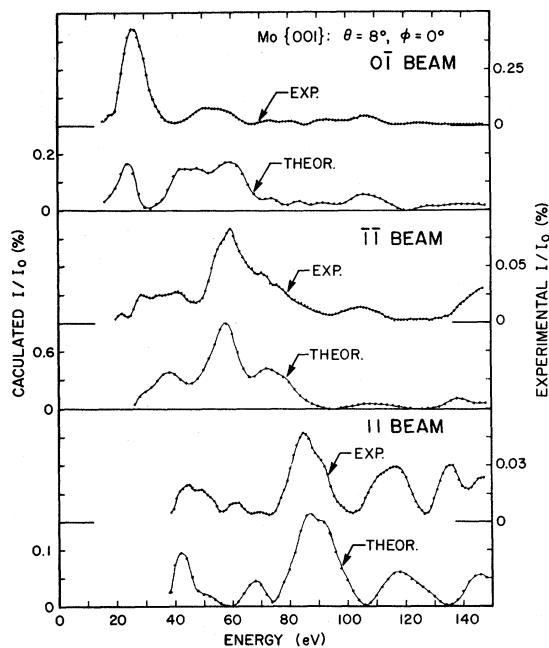


FIG. 10. Experimental and theoretical spectra (calculated with the parameters listed in the text) for clean Mo{001} at  $\theta = 8^\circ$ ,  $\phi = 0^\circ$ ;  $0\bar{1}$ ,  $\bar{1}\bar{1}$ , 11 beams.

calculated for a constant value of  $V_0^B$  with the peak positions in the corresponding experimental spectrum. The results for all major peaks in all beams considered in this analysis fluctuate around a mean curve that represents the energy dependence of the bulk inner potential  $V_0^B$ . Figure 8 depicts such a curve. Accordingly, an energy-dependent  $V_0^B$ , as determined from the solid curve in Fig. 8, was introduced in the calculations. The corresponding surface quantity  $V_0^S$  was varied by as much as 5 eV on either side of  $V_0^B$ , but no value was found that would improve the theory-experiment agreement beyond that obtained for  $V_0^S = V_0^B$ .

The final results are displayed in Figs. 9 and 10 for the six beams measured experimentally at  $\theta = 8^\circ$ ,  $\phi = 0^\circ$ . At this stage of the analysis, all available structural and nonstructural parameters having been fixed, the spectra of the beams measured at  $\theta = 21^\circ$  were calculated. The results are compared with experiment in Fig. 11. The correspondence between observations and calculations is not as good as at  $\theta = 8^\circ$ . Reconsideration of all parameter values did not produce better results. Whenever a parameter value was found that would slightly improve the  $21^\circ$  data, the same value was found to worsen unacceptably the  $8^\circ$  results. The results presented in Fig. 11 are therefore considered final: Although not as good as at  $8^\circ$ , the correspondence between theory and experiment is satisfactory, particularly at energies higher than about 40 eV.

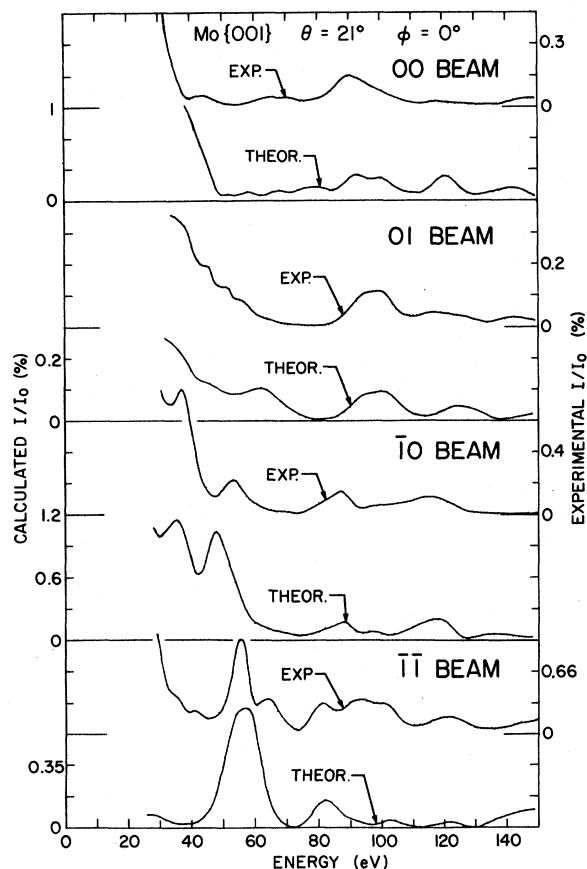


FIG. 11. Experimental and theoretical spectra (calculated with the parameters listed in the text) for clean Mo{001} at  $\theta = 21^\circ$ ,  $\phi = 0^\circ$ : 00,  $\bar{1}0$ , 01,  $\bar{1}\bar{1}$  beams.

#### IV. CONCLUSIONS AND DISCUSSION

The list of parameters that represent the final structural model of the clean Mo{001} surface is the following:  $d_z^S = 1.39 \text{ \AA}$ ,  $\beta^B = \beta^S = 4 \text{ eV}$ ,  $V_0^B = V_0^S$  variable with energy as depicted in Fig. 8,  $\Theta_D^B = 360 \text{ }^\circ\text{K}$ ,  $\Theta_D^S = 150 \text{ }^\circ\text{K}$ . The overall correspondence between observations and calculations within two sets of data at two different angles of incidence for a total of ten nondegenerate beams is considered satisfactory. No explanation was found for the fact that the correspondence is less good at large incidence angles than at small. Although a trend in this direction could possibly have been recognized in the early and unrefined structure analysis of aluminum surfaces,<sup>21</sup> it was so far not confirmed in the analyses of clean-surface structures of other materials.<sup>11,22</sup> It is more probable that the high-

angle experimental data reported here were somehow affected by the incident reported above that caused buckling of the sample surface.

The results of the present work indicate that the clean Mo{001} surface is contracted by about 11.5% with respect to the bulk. The magnitude of this contraction seems at first sight to be large, certainly larger than any contraction or expansion reported so far for other metal surfaces.<sup>1</sup> Since this result is based predominantly on the analysis of one spectrum (the 10 beam at  $\theta = 8^\circ$ , see above), all other spectra considered here being rather insensitive to the value of  $d_z^S$ , a few remarks may be appropriate.

The interplanar distance  $d_z^S = 1.39 \text{ \AA}$  corresponds to a Mo-Mo nearest-neighbor interatomic distance along the  $\langle 111 \rangle$  direction of  $2.62 \text{ \AA}$ , to be compared with the Mo-Mo interatomic distance within the bulk of  $2.72 \text{ \AA}$ . Thus, the interatomic distance is reduced only by 3.7% in the Mo{001} surface. The changes reported in the literature for the interplanar distance found in metal surfaces concern exclusively fcc metals, the present work being the first concerned with a bcc metal. It is a consequence of the more close-packed nature of the fcc structure, that a given change in the  $\langle 001 \rangle$  interplanar spacing causes a larger change in the interatomic distance than in the bcc structure. For example, a change of 10% in the interplanar spacing along  $\langle 001 \rangle$  causes a change of about 5% in the interatomic distance in fcc structures, but only a change of about 3% in the interatomic distance in bcc structures. From this point of view, the contraction of Mo{001} reported here does not appear as exaggerated as it may at first sight. It may also be interesting to point out that this contraction does not persist when foreign atoms are adsorbed on the Mo{001} surface.<sup>23</sup>

#### ACKNOWLEDGMENTS

Three of the authors (A. Ignatiev, F. Jona, and H. D. Shih) would like to express their appreciation for the partial support of this work provided by the Air Force Office of Scientific Research, Air Force Systems Command, under Grant No. AFOSR-72-2151, in the initial stages; and by the National Science Foundation, under Grant HO-37956, in the final stages. Assistance, help and advice of K. O. Legg are also gratefully acknowledged. C. H. Huang and P. J. Estrup of Brown University were very helpful to us in the early stages of this work by allowing us to compare some of our LEED spectra for the clean Mo{001} surface with theirs.

\* Present address: Department of Physics, University of Houston, Houston, Tex. 77004.

<sup>1</sup>See, e.g., the review article by J. A. Strozier, Jr.,

D. W. Jepsen, and F. Jona, in *Surface Physics of Crystalline Materials*, edited by J. M. Blakely (Academic, New York, 1975).

- <sup>2</sup>F. Jona and H. R. Wendt, *Rev. Sci. Instrum.* **40**, 1172 (1969).
- <sup>3</sup>N. Laegreid and G. K. Wehner, *J. Appl. Phys.* **32**, 365 (1961).
- <sup>4</sup>After completion of the experimental part of this work, a paper by Lecante *et al.* appeared in the literature that describes somewhat similar cleaning procedures for Mo{001} as described above. [J. Lecante, R. Riwan, and C. Guillot, *Surf. Sci.* **35**, 271 (1973)].
- <sup>5</sup>D. Tabor, J. M. Wilson, and T. J. Bastow, *Surf. Sci.* **26**, 471 (1971).
- <sup>6</sup>T. W. Haas, J. T. Grant, and G. J. Dooley, *Phys. Rev. B* **1**, 1449 (1970).
- <sup>7</sup>F. Jona, *IBM J. Res. Dev.* **14**, 444 (1970).
- <sup>8</sup>U. V. Azizov, V. V. Vakhidov, V. M. Sulmanov, B. N. Sheinberg, and G. N. Shuppe, *Fiz. Tverd. Tela* **7**, 2759 (1965) [*Sov. Phys. -Solid State* **7**, 2232 (1966)].
- <sup>9</sup>D. W. Jepsen and P. M. Marcus, in *Computational Methods in Band Theory*, edited by P. M. Marcus, J. F. Janak, and A. R. Williams (Plenum, New York, 1971), pp. 416-443.
- <sup>10</sup>D. W. Jepsen, P. M. Marcus, and F. Jona, *Phys. Rev. B* **5**, 3933 (1972).
- <sup>11</sup>D. W. Jepsen, P. M. Marcus, and F. Jona, *Phys. Rev. B* **8**, 5523 (1973).
- <sup>12</sup>A. U. MacRae and L. H. Germer, *Phys. Rev. Lett.* **8**, 489 (1962).
- <sup>13</sup>A. U. MacRae, *Surf. Sci.* **2**, 522 (1964).
- <sup>14</sup>R. M. Goodman, H. H. Farrell, and G. A. Somorjai, *J. Chem. Phys.* **48**, 1046 (1968).
- <sup>15</sup>H. B. Lyon and G. A. Somorjai, *J. Chem. Phys.* **44**, 3707 (1966).
- <sup>16</sup>C. Corotte, P. Ducros, and A. Mascall, *C. R. (Paris)* **B267**, 544 (1968).
- <sup>17</sup>A. Ignatiev and T. N. Rhodin, *Phys. Rev. B* **8**, 893 (1973).
- <sup>18</sup>F. R. Jones, J. T. McKinney, and M. B. Webb, *Phys. Rev.* **151**, 476 (1966).
- <sup>19</sup>D. W. Jepsen, P. M. Marcus, and F. Jona, *Surf. Sci.* **41**, 223 (1974).
- <sup>20</sup>A. Ignajevs, T. N. Rhodin, S. Y. Tong, B. I. Lundqvist, and J. B. Pendry, *Solid State Commun.* **9**, 1851 (1971).
- <sup>21</sup>D. W. Jepsen, P. M. Marcus, and F. Jona, LEED 5, Lecture Notes, National Bureau of Standards, March 18-19, 1971, p. 1 (unpublished).
- <sup>22</sup>Agreement between observations and calculations is found to be excellent for angles of incidence as high as 24° on clean Ti(0001) and clean Fe(001) surfaces [H. D. Shih, K. O. Legg, F. Jona, D. W. Jepsen, and P. M. Marcus (unpublished)].
- <sup>23</sup>A. Ignatiev, F. Jona, D. W. Jepsen, and P. M. Marcus, *J. Vac. Sci. Technol.* **12**, 226 (1974); and preceding paper, *Phys. Rev. B* **11**, 4780 (1975).